

BEHAVIOUR OF REINFORCED CONCRETE BEAMS WITHOUT STIRRUPS SUBJECTED TO STEEL REINFORCEMENT CORROSION

Rizwan AZAM^{a, c}, Ahmed K. EL-SAYED^b, Khaled SOUDKI^a

^aDepartment of Civil Engineering, University of Waterloo, Waterloo, ON, Canada

^bDepartment of Civil Engineering, King Saud University, Riyadh, KSA

^cDepartment of Civil Engineering, University of Engineering & Technology Lahore, Pakistan

Received 22 Jan 2013; accepted 08 Apr 2013

Abstract. The effect of corrosion on the structural behaviour of reinforced concrete (RC) beams without stirrups was experimentally investigated. A total of seven medium-scale RC beams without stirrups were constructed. The beams measured 150 mm wide, 250 mm deep and 1700 mm long. The test variables included: three different longitudinal reinforcement ratios (0.91%, 1.21%, and 1.82%) and two different corrosion levels (3% and 10%). Four beams were subjected to artificial corrosion whereas three beams acted as control un-corroded. Following the corrosion phase, all beams were tested to failure in three point bending. Corrosion crack widths and cracking patterns were recorded at different stages of corrosion. The effect of different longitudinal reinforcement ratios on the rate of corrosion was observed. Test results revealed that the beams with higher reinforcement ratios experienced slower corrosion rate compared to beams with lower reinforcement ratios. All control beams failed in shear whereas corroded beams failed in bond. There was a significant reduction in the load carrying capacity of the corroded beams without stirrups compared to the control beams.

Keywords: corrosion, shear, bond, reinforced concrete.

Introduction

Corrosion of reinforcing steel is the most significant deterioration problem faced by reinforced concrete (RC) structures. The US State Department has spent an estimated \$5 billion to remediate concrete bridges in US for the year 2000, which were directly affected by corrosion of their reinforcing steel bars (Newman, Chow 2003). Similar costs are spent in Europe and Canada to maintain their bridge infrastructure in service. To efficiently rehabilitate corrosion damaged reinforced concrete structures, the residual strength and failure mechanism of the deteriorated structures must be determined. For this purpose, a number of studies have been reported in the literature. The majority of studies in the literature focused on flexural and bond strength of corroded RC beams (Al-Sulaimani *et al.* 1990; Almusallam *et al.* 1996; Mangat, Elgarf 1999). Models have been developed by many researchers to determine the residual flexural/bond strength of corroded RC beams (Wang, Liu 2006; Bhargava *et al.* 2007; Azad *et al.* 2007). However, there are only a few studies related to the shear strength of corroded RC beams.

At present, structures are facing corrosion problems after thirty to forty years of their service life. These structures were designed based on design codes prevailing

three to four decades ago. Recent studies (Sneed 2007; Sherwood *et al.* 2006) related to size effect on shear strength of members have indicated that the shear strength of members designed three to four decades ago was overestimated. In addition, the code conditions at that time for provisions of stirrups were not as stringent as codes today. As a result, a large number of structures in service are without stirrups, having a minute margin of safety. For instance, the partial collapse of Viaduc de la Concorde overpass in 2006 in Laval, Quebec highlighted this problem. Besides, a recent literature survey (Collins *et al.* 2008), related to the shear strength of members constructed without stirrups, has indicated that there are structures in service with higher probability of experiencing a shear failure. Therefore, it is of great importance to study the effect of corrosion on shear strength of RC beams without shear reinforcement.

A number of studies (Azam, Soudki 2013, 2012; Xue, Seki 2010; Toongonthong, Meakawa 2004; Satoh *et al.* 2003; Cairns 1995; Raof, Lin 1997) have been reported in the literature on effect of corrosion on behaviour of RC beams without stirrups. However, these studies assumed proper anchorage of the reinforcement but there may be conditions in service when anchorage

is also impaired due to corrosion. This study is focused on investigating the load carrying capacity of corroded RC beams without stirrups of which anchorage is also impaired due to corrosion.

1. Research significance

Shear failure is brittle in nature and should be avoided. Concrete beams without stirrups generally fail in this mode of failure. These members are expected to experience reduced load carrying capacity less than their design capacity due to corrosion of the flexural reinforcement. This study investigates the failure mechanism and residual strength of reinforced concrete beams without stirrups damaged due to corrosion of their longitudinal bars. This study will provide experimental data that will be useful in designing efficient repair systems for such damaged beams.

2. Experimental program

A total of seven beams were constructed and tested. Four beams were subjected to accelerated corrosion and the remaining three beams were kept as control without corrosion. All beams were without compression and transverse shear reinforcement. Test variables included the amount of longitudinal reinforcement ratio (0.91%, 1.21% and 1.82%) and the level of corrosion (none, light and medium). Table 1 summarizes the test matrix.

2.1. Test setup and instrumentation

The details of the test specimens are presented in Figure 1. All beams were 150 mm wide, 250 mm deep and 1700 mm long. The beams were reinforced with 3-10M, 2-15M and 2-20M bars. The shear span and effective depth were kept constant at 700 mm and 220 mm respectively, to give a constant shear span to depth ratio of 3.2. The test beams were divided into three series: A, B and C. Series-A had three beams, one control and two corroded. Series-B and C had two beams, one control and one corroded. Each beam was designated with a

Table 1. Test matrix

Series	Beam designation	Target f'_c (MPa)	Longitudinal reinforcement			
			Type of rebar	ρ (%)	ρ/ρ_b	Corrosion level
A	N-0.91	40	3-10M	0.91	0.21	None
	L-0.91	40	3-10M	0.91	0.21	Light
	M-0.91	40	3-10M	0.91	0.21	Medium
B	N-1.21	40	2-15M	1.21	0.28	None
	M-1.21	40	2-15M	1.21	0.28	Medium
C	N-1.82	40	2-20M	1.82	0.42	None
	M-1.82	40	2-20M	1.82	0.42	Medium

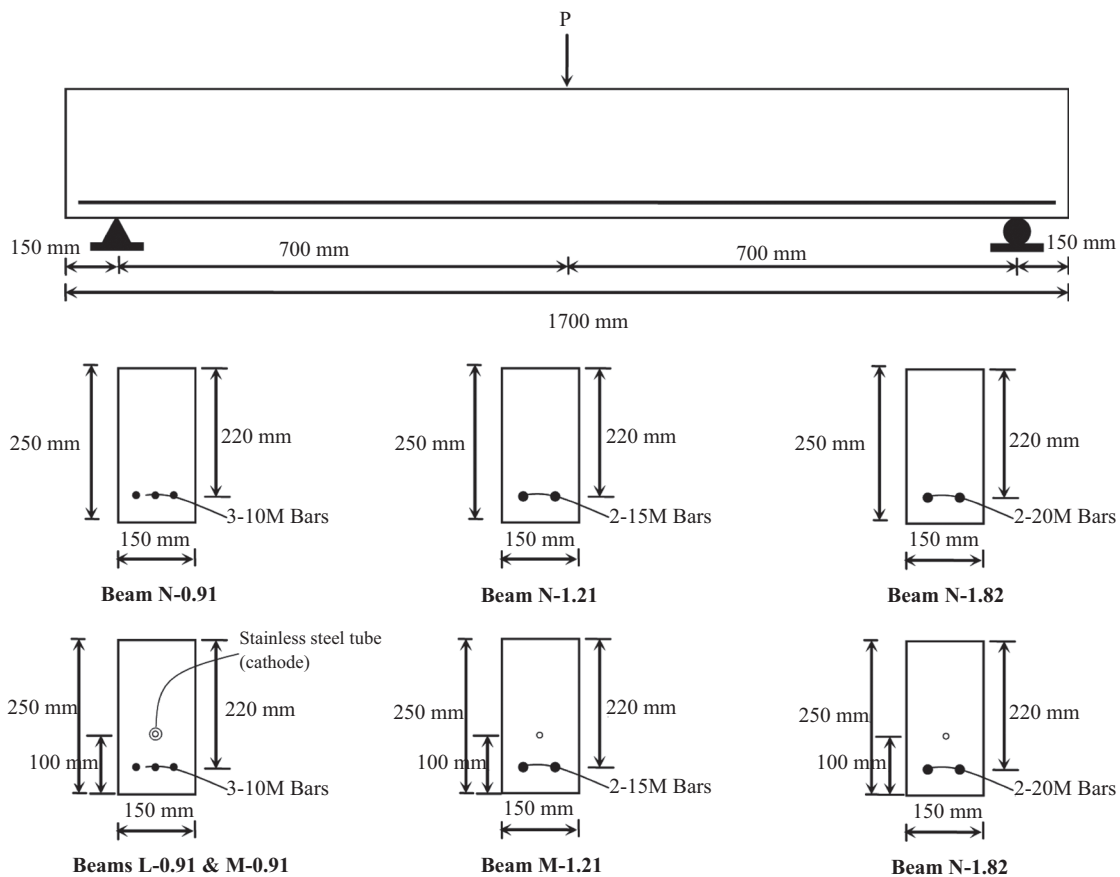


Fig. 1. Details of test specimens and loading arrangement

letter and a number: the letter indicating the corrosion level (N = None, L = Light and M = Medium) and the number indicating the reinforcement ratio.

The beams subjected to corrosion were cast with salted concrete up to a depth of 100 mm and the remaining beam depth was cast with unsalted concrete. A 9.5 mm diameter Type 304 stainless hollow steel tube, which acts as a cathode in the accelerated corrosion setup, was placed at 100 mm from bottom in all four beams subjected to corrosion. The control beams were cast with unsalted concrete. All three control beams, one from each series, were instrumented with 5 mm electrical 120 Ω resistance strain gauges bonded to the reinforcing bar at mid-span.

2.2. Materials

The concrete used for construction of these beams was supplied by a local ready-mix concrete supplier. The concrete was batched with Type-10 Portland cement; the maximum coarse aggregate size was 19 mm. The concrete was batched at a water cementing material ratio of 0.45.

A measured volume of concrete was removed from the concrete transit mix truck and water containing salt was added and the salted concrete was mixed in the laboratory. The amount of water added was calculated to adjust the water cementing ratio from 0.45 to 0.55 and the amount of salt added was calculated having 2.3% chlorides by mass of cement. Water was also added to the remaining concrete in the truck to adjust its water cementing material ratio from 0.45 to 0.55.

A total of fourteen concrete cylinders (100×200 mm) were also cast from the same concrete batch. At the time of beam testing, the average compressive strength of the concrete was 42.6±1.37 MPa.

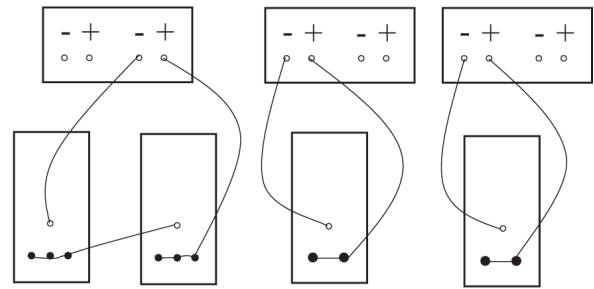
Grade 400 reinforcing steel bars were used to reinforce the concrete beams. Three different bar sizes were used: 10M, 15M and 20M. The cathode stainless steel tube was type 304 with an outside diameter of 9.5 mm and a wall thickness of 0.89 mm.

2.3. Accelerated corrosion

After 28 days of curing, four beams (L-0.91, M-0.91, M-1.21 and M-1.81) were subjected to accelerated corrosion by impressing a direct current into the bars through power supplies; one power supply for each series. Beams L-0.91 and M-1.21 were connected in series to one power supply. Separate power supplies were used for beams M-1.21 and M-1.81.

The reinforcing bar acted as an anode and the stainless steel tube acted as a cathode in this artificial corrosion cell. The schematic diagram showing the details of the connection between the reinforcing bars, the stainless steel tube and the power supply is shown in Figure 2.

The direct current was impressed through the reinforcing bars at a constant current density. A current density of 200 $\mu\text{A}/\text{cm}^2$ was selected, based on a study done by El-Maaddawy and Soudki (2003), to corrode the



Beam L-0.91 Beam M-0.91 Beam M-1.21 Beam M-1.82

Fig. 2. Details of accelerated corrosion circuit

beams in a reasonable time period and to have similar corrosion products and cracking as those found in field.

To disrupt the passive layer around the reinforcing bar embedded in the concrete, salt was mixed in concrete during casting of the beams. The moisture and air required for corrosion reactions, was provided by a mist nozzle. The nozzle was connected to a water tap and pressurized air tap. To maintain the humid environment around the beams, they were placed on frames and covered with plastic sheets.

The time required for corroding the reinforcing steel bars to light corrosion level (3%) and medium corrosion level (10%) was calculated based on Faraday's law. After reaching a light corrosion level, beam L-0.91 was removed from the corrosion chamber. The other three beams (M-0.91, M-1.21 and M-1.82) remained in the chamber until theoretically reaching the medium corrosion level.

2.4. Test setup and procedure

The beams were tested in three point bending. The beams were simply supported, over a clear span of 1400 mm with one concentrated load at mid-span as shown schematically in Figure 1 and photographically in Figure 3. The load was applied at a stroke rate of 0.3 mm/min. using a material testing frame with maximum capacity of 155 KN. The beam mid-span deflection was measured using a linear variable differential transformer (LVDT) with a range of ±25 mm. The applied load, displacements



Fig. 3. Test setup

crack is initiated. In all beams the thickness of concrete ring is governed by the bottom cover which is less as compared to side cover, which means cracks will appear on the bottom face. But in beams L-0.91 and M-0.91 which are reinforced with three bars the concrete rings for different bars overlaps with each other in horizontal direction, which leads to excessive pressures in horizontal direction and hence to horizontal cracks. The theoretical cracking pattern due to corrosion of the reinforcing bars in the test beams is shown schematically in Figure 5.

3.2. Reinforcing steel mass loss

To determine the actual mass loss, bars were carefully extracted from the corroded beams following the load testing phase. The procedure given in standard ASTM GI-03 (2011), designation C.3.5 was used for the mass loss analysis. Twelve coupons, four from each bar, of 300 mm length were taken from beams L-0.91 and M-0.91 and eight coupons, four from each bar, of the same length were taken from beams M-1.21 and M-1.82. Coupons from the control beams were used as a reference.

The comparison of theoretical and experimental mass losses is given in Table 2. Key findings from the mass loss data are: for lower mass losses, Faraday's law underestimates the mass losses; whereas for higher mass losses it overestimates the steel mass loss due to corrosion. This is explained in the following. At early stages of corrosion (lower corrosion level) the cracks are opened and oxygen and water can easily reach the bar to accelerate the corrosion whereas at later stages of corrosion (higher corrosion level) the corrosion products build up around the bar and fill the cracks, thus reducing the concentration of oxygen and water around the bar, which ultimately slows down the corrosion rate.

For beams with lower reinforcement ratios, Faraday's law gives approximately comparable mass loss re-

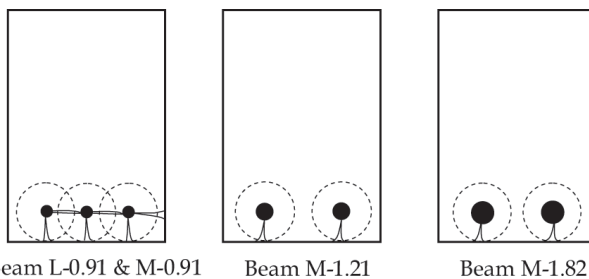


Fig. 5. Theoretical cracking patterns

Table 2. Comparison of theoretical and experimental mass losses

Beam	Theoretical mass loss (%)	Experimental mass loss (%)
L-0.91	3	5.4±2.09
M-0.91	10	9.7±0.92
M-1.21	10	8.01±0.98
M-1.82	10	7.17±0.37

sults whereas for beams with higher reinforcement ratios it overestimates the steel mass loss due to corrosion. At a given corrosion level, the steel mass loss in grams for 3-10M bars (the beam with reinforcement ratio of 0.91%) is less than that for the 2-15M and 2-20M bars (the beams with reinforcement ratios of 1.21% and 1.82% respectively), which means that for beams with higher reinforcement ratios the pores and cracks around the bar will be filled with corrosion products earlier than the beams with lower reinforcement ratios resulting in slowing down the movement of oxygen and water to the bar surface, which result in reduced corrosion rate for such beams.

The corrosion mass loss was uniformly distributed with exception of few pits along the length of the bars indicating uniform corrosion. The effect of corrosion on reinforcing bars in terms of penetration depth (reduction in bar radius) is presented in Table 3.

3.3. Structural behaviour

The load deflection response of all the beams is shown in Figure 6. A summary of the test results along with the predicted ultimate strengths of the control beams using ACI 318-08 (2008) and CSA A23.3-04 (2010) is given in Table 4. Typical load deflection response can be described by three distinct stages; the first stage represents the behaviour of an un-cracked beam with gross moment of inertia, the second stage represents the behaviour of a cracked beam with reduced moment of inertia and the third stage is the post peak stage after failure. The behaviour of all beams was approximately similar before cracking (first stage) but, there was a significant reduction in the stiffness of corroded beams after cracking (second stage). The post peak stage of corroded beams was a gradual drop in the load carrying capacity as compared to the control beam which exhibits sudden drop at onset of failure.

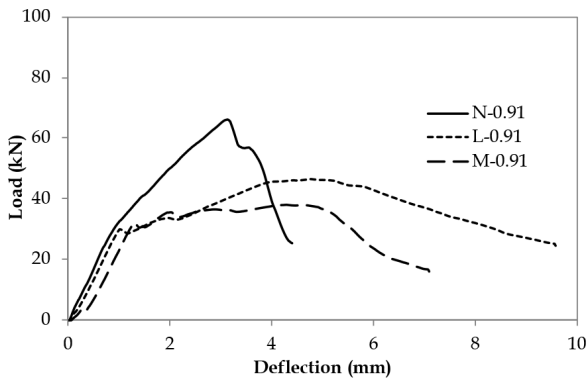
Figure 6 shows that the corroded beams experienced significant loss of stiffness after cracking. The stiffness loss is mainly due to horizontal cracking leading to bond failure. The stiffness loss in beam L-0.91 (low corrosion) and M-0.91 (medium corrosion) was approximately 70% and 90% respectively compared to the stiffness in beam N-0.91 (no corrosion). The reduction in the stiffness in beams M-1.21 and M-1.82 (medium corrosion) was 75% and 65%, respectively. The comparison of the stiffness of all corroded beams indicates that stiffness degradation increased with corrosion level and that the beams with higher reinforcement ratios experienced lesser

Table 3. Corrosion attack penetration values

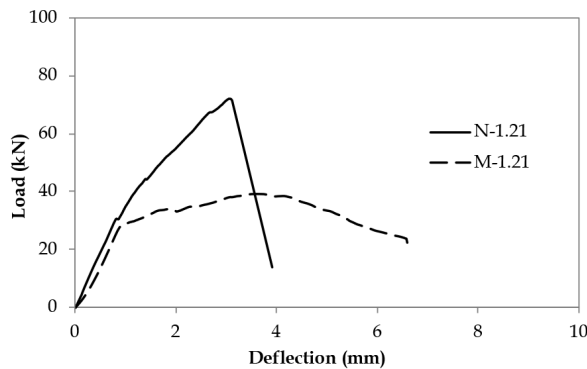
Beam	Corrosion attack penetration (mm)
L-0.91	0.15
M-0.91	0.28
M-1.21	0.32
M-1.82	0.35

Table 4. Summary of test results

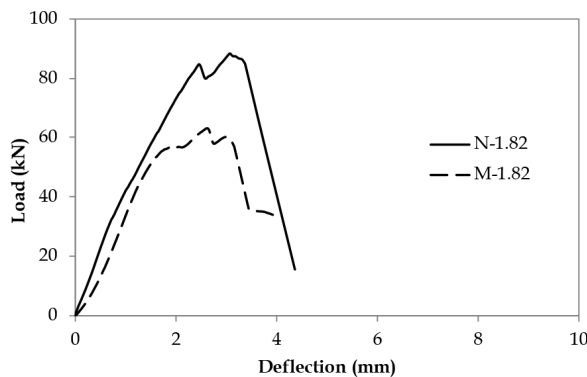
Series	Beam designation	Predicted ultimate load by CSA A23.3-04 (kN)	Predicted ultimate load by ACI 318-08 (kN)	Experimental load		Reduction in ultimate load (%)	Deflection at ultimate load (mm)	Maximum strain in steel rebar ($\mu\epsilon$)	Failure mode
				Inclined cracking load (kN)	Ultimate load (kN)				
A	N-0.91	61.2	69.79	65	66.13	–	3.13	1933	Shear
	L-0.91	–	–	–	46.32	30	4.76	–	bond
	M-0.91	–	–	–	37.98	42.6	4.28	–	bond
B	N-1.21	68.3	70.07	69	72.02	–	3.06	1761	Shear
	M-1.21	–	–	–	39.30	45.4	3.57	–	bond
C	N-1.82	79	70.65	80	88.52	–	3.08	1421	Shear
	M-1.82	–	–	–	63.18	28.6	2.62	–	bond



(a)



(b)



(c)

Fig. 6. Load deflection behaviour of tested beams: a) series-A; b) series-B; c) series C

reduction. The larger reduction in stiffness in beams L-0.91 and M-0.91 is mainly due to initial horizontal cracks in these beams due to corrosion. The lesser reduction in stiffness with higher reinforcement ratios was possibly due to lower corrosion levels observed in these beams.

The reduction in stiffness after cracking in the corroded beams causes excessive deflections. In order to quantify this effect, the deflection at maximum load in the corroded beams was compared with deflection at same load in the control beams. The deflection at maximum load in beam L-0.91 (low corrosion) was 4.76 mm compared to a deflection of 1.78 mm in beam N-0.91 (no corrosion) at same load level (46 kN), which was around 2.5 times higher. The deflection in beam M-0.91 (medium corrosion) was 4.28 mm compared to a deflection of 1.29 mm in beam N-0.91 (no corrosion), which was more than three times higher. The increase in deflection in beams M-1.21 and M-1.82 was around three times (from 1.16 mm in N-1.21 to 3.57 mm in M-1.21) and 1.5 times (from 1.96 mm in N-1.82 to 2.62 in beam M-1.82), respectively. Thus, as corrosion level increases the beam deflection increased. Beams with higher reinforcement ratios experience relatively less increase in deflection.

The typical failure mode of the control and corroded beams is shown in Figure 7. The control beams failed abruptly in shear indicating the brittle nature of this type of failure. The maximum strains in the tension steel reinforcement at failure in control beams N-0.91, N-1.21 and N-1.82 (respectively 1933, 1761 and 1421 micro strain) were lower than the yield strain of steel reinforcement (2000 micro strains). The cracking in the control beams was initiated with the appearance of cracks at mid-span under the concentrated load. As the load increased, an inclined crack appeared in the shear span which progressed towards the load point and the support, leading to a diagonal tension failure (Fig. 7a). The corroded beams failed by bond as shown in Figure 7b. The failure mode was a progressive failure unlike the sudden shear failure experienced by the control (un-corroded) beam. The cracking was initiated with the appearance of flexural cracks at mid span. As load increased, flexural cracking progressed

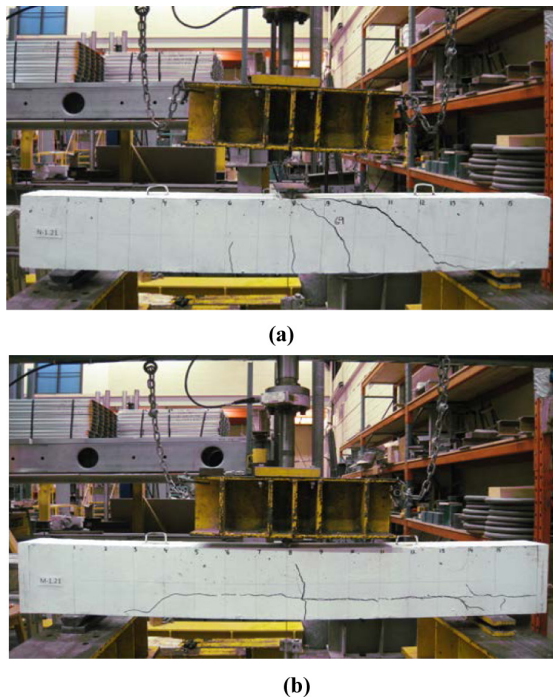


Fig. 7. Failure modes: a) Control beam (N-1.21); and b) Control beam (M-1.21)

towards the compression zone and later horizontal cracking appeared close to mid span and progressed towards the support, leading to a bond failure.

All control beams failed suddenly after the formation of inclined or diagonal cracking. The difference between the inclined cracking load and the ultimate load ranged between 2 to 9% for the low (0.91%) to high (1.82%) reinforcement ratio, respectively. For higher reinforcement ratios the strain in the steel reinforcement at failure was less than that in beams with lower reinforcement ratio. This helped in keeping the inclined cracks closed.

The ultimate shear capacity of the control beams increased with increase in the reinforcement ratio. The increase in ultimate shear capacity was about 34% as the reinforcement ratio increased from 0.91% to 1.81%. The increase in shear strength with higher reinforcement ratio is due to the improvement in the shear transfer mechanisms; shear stresses in the un-cracked concrete, interface shear transfer and dowel action.

The effect of corrosion on the load carrying capacity of the beam with different levels of corrosion in series A beams is shown in Figure 8. The load carrying capacity decreased as corrosion level increased. The reduction for beams L-0.91 and M-0.91 was 30% and 42.6%, respectively. These beams failed by bond and thus the bond strength decreases as corrosion level increases.

The effect of corrosion on load carrying capacity of beams with different reinforcement ratios is shown in Figure 9. It is evident that the reduction in load carrying capacity due to corrosion for beams with reinforcement ratios of 0.91% and 1.21% was on average 44%. On the other hand, the capacity for the beam with reinforcement

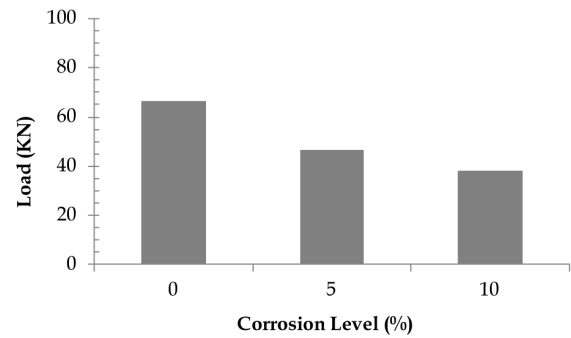


Fig. 8. Effect of corrosion level on load carrying capacity of series A beams

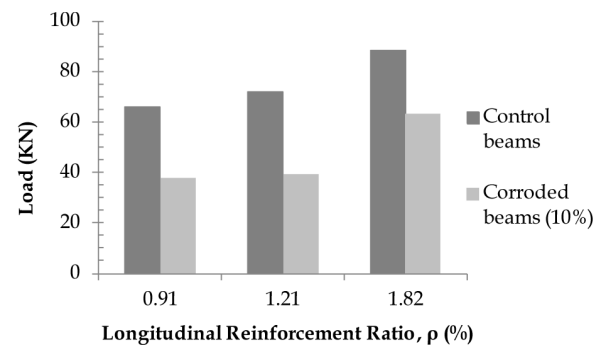


Fig. 9. Effect of corrosion on load carrying capacity of beams with different reinforcement ratios

ratio of 1.82% was reduced by 28% due to corrosion. The lower reduction in the load carrying capacity in the beam with 1.82% reinforcement ratio was possibly due to the lower corrosion level attained by this beam. The measured mass loss for the reinforcing bars in beam M-1.82 was on average 20% lower than those in beams M-0.91 and M-1.21 (Table 2), even though all three beams were subjected to same induced corrosion level.

Conclusions

The following conclusions are made based on the results of this study:

- The cracking pattern due to corrosion is affected by the number of bars being corroded. The beams with clear bar spacing less than twice the concrete cover to bar diameter experiences horizontal cracking which is worse for bond. It is recommended to keep the bar spacing between bars equal or greater than twice the concrete cover wherever possible.
- The rate of corrosion was slower in beams with higher reinforcement ratios compared to beams with smaller reinforcement ratios.
- It is expected that the beams with higher reinforcement ratios will experience lower reduction in load carrying capacity compared to beams with lower reinforcement ratios.
- Corrosion of longitudinal reinforcement caused the mode of failure in the beams to change from shear to bond failure.

- The reduction in load carrying capacity increased as corrosion level increased. At 10% corrosion level, the load carrying capacity was 55% of the capacity of the un-corroded beam.

Acknowledgements

The authors would like to acknowledge the financial support received from University of Engineering and Technology Lahore, Pakistan. The financial support received from the Natural Sciences and Engineering Research Council (NSERC) is also acknowledged. The donation of the concrete from Hogg Ready Mix is appreciated. The help in laboratory work provided by the University of Waterloo technicians and the other members of the rehabilitation research group at the University of Waterloo is greatly appreciated.

References

- ACI 318-08. Building code requirements for structural concrete (ACI 318-08) and commentary.* American Concrete Institute. 2008.
- Almusallam, A. A.; Al-Gahtani, A. S.; Aziz, A. R.; Rasheeduzzafar. 1996. Effect of reinforcement corrosion on bond strength, *Construction and Building Materials* 10(2): 123–129. [http://dx.doi.org/10.1016/0950-0618\(95\)00077-1](http://dx.doi.org/10.1016/0950-0618(95)00077-1)
- Al-Sulaimani, G. J.; Kaleemullah, M.; Basunbul, I. A.; Rasheeduzzafar. 1990. Influence of corrosion and cracking on bond behaviour and strength of reinforced concrete members, *ACI Structural Journal* 87(2): 220–231.
- ASTM G1-03. Standard practice for preparing, cleaning and evaluating test specimens.* ASTM International, West Conshohocken, PA. 2011.
- Azad, A. K.; Ahmad, S.; Azher, S. A. 2007. Residual strength of corrosion damaged reinforced concrete beams, *ACI Materials Journal* 104(1): 40–47.
- Azam, R.; Soudki, K. 2012. Structural performance of shear critical RC deep beams with corroded longitudinal steel reinforcement, *Cement and Concrete Composites* 34(8): 946–957. <http://dx.doi.org/10.1016/j.cemconcomp.2012.05.003>
- Azam, R.; Soudki, K. 2013. Structural behaviour of shear-critical RC slender Beams with corroded properly anchored longitudinal steel reinforcement, *Journal of Structural Engineering* ASCE 139(12). [http://dx.doi.org/10.1061/\(ASCE\)ST.1943-541X.0000799](http://dx.doi.org/10.1061/(ASCE)ST.1943-541X.0000799)
- Bhargava, K.; Ghosh, A. K.; Mori, Y.; Ramanujam, S. 2007. Models for corrosion-induced bond strength degradation in reinforced concrete, *ACI Structural Journal* 104(6): 594–603.
- CSA A23.3-04. Design of concrete structures.* Canadian Standards Association. 2010.
- Cairns, J. 1995. Strength in shear of concrete beams with exposed reinforcement, in *Proceedings of the Institution of Civil Engineers - Structures and Buildings* 110(2): 176–185. <http://dx.doi.org/10.1680/istbu.1995.27598>
- Collins, M. P.; Bentz, E. C.; Sherwood, E. G. 2008. Where is shear reinforcement required? A review of research results and design procedures, *ACI Structural Journal* 105(5): 590–600.
- El-Maaddawy, T. A.; Soudki, K. A. 2003. Effectiveness of impressed current technique to simulate corrosion of steel reinforcement in concrete, *Journal of Materials in Civil Engineering* ASCE 15(3): 41–47. [http://dx.doi.org/10.1061/\(ASCE\)0899-1561\(2003\)15:1\(41\)](http://dx.doi.org/10.1061/(ASCE)0899-1561(2003)15:1(41))
- El-Maaddawy, T. A.; Soudki, K. A. 2007. A model for prediction of time from corrosion initiation to corrosion cracking, *Cement and Concrete Composites* 29(3): 168–175. <http://dx.doi.org/10.1016/j.cemconcomp.2006.11.004>
- Mangat, P. S.; Elgarf, M. S. 1999. Flexural strength of concrete beams with corroding reinforcement, *ACI Structural Journal* 96(1): 149–158.
- Newman, J.; Chow, B. S. 2003. *Advanced concrete technology 2: concrete properties.* Butterworth-Heinemann. 352 p.
- Raouf, M.; Lin, Z. 1997. Structural characteristics of RC beams with exposed main steel, in *Proceedings of the Institution of Civil Engineers - Structures and Buildings* 122(1): 35–51. <http://dx.doi.org/10.1680/istbu.1997.29166>
- Satoh, Y., et al. 2003. Shear behaviour of RC member with corroded shear and longitudinal reinforcing steel, in *Proceedings of the JCI* 25(1): 821–826.
- Sherwood, E. G.; Lubell, A. S.; Bentz, E. C.; Collins, M. P.; 2006. One way shear strength of thick slabs and wide beams, *ACI Structural Journal* 103(6): 180–190.
- Sneed, L. H. 2007. *Influence of member depth on shear strength of concrete beams:* PhD thesis. Purdue University, West Lafayette, Indiana.
- Toongeonhong, K.; Meakawa, K. 2004. Interaction of pre-induced damages along the main reinforcement and diagonal shear in RC members, *Journal of Advanced Concrete Technology* 2(3): 431–443.
- Wang, X.; Liu, X. 2006. Bond strength modeling for corroded reinforcements, *Construction and Building Materials* 20: 177–186. <http://dx.doi.org/10.1016/j.conbuildmat.2005.01.015>
- Xue, X.; Seki, H. 2010. Influence of longitudinal bar corrosion on shear behaviour of RC beams, *Journal of Advanced Concrete Technology* 8(2): 145–156.

Rizwan AZAM. He is a PhD candidate in the Department of Civil and Environmental Engineering at the University of Waterloo, Waterloo, Ontario, Canada. He is an Assistant Professor (on Leave) in the Department of Civil Engineering at University of Engineering & Technology Lahore, Pakistan, where he received his BS in Civil Engineering in 2007. He received his MS from the University of Waterloo, Waterloo, Ontario, Canada in 2010. His research interest includes computer aided design of structures and the assessment and rehabilitation of reinforced concrete structures.

Ahmad K. EL-SAYED. He is an Associate Professor in the Centre of Excellence for Concrete Research and Testing at King Saud University, Riyadh, Saudi Arabia. He received his PhD from the University of Sherbrooke, Sherbrooke, QC, Canada. His research interests include corrosion, rehabilitation and reinforcing of concrete structures using FRP composites. He is an associate professor (on leave) in the Housing and Building National Research Center, Giza, Egypt.

Khaled SOUDKI. He is a Professor and Canada Research Chair in Innovative Structural Rehabilitation at the University of Waterloo. He is a Member of ACI Committees 222, Corrosion of Metals in Concrete; 440, Fiber Reinforced Polymer Reinforcement; and 546, Repair of Concrete; and Joint ACI-ASCE Committee 550, Precast Concrete Structures. His research interests include corrosion, durability, rehabilitation, and reinforcing of concrete structures using fiber-reinforced polymer composites.